Communication

Diffusion and Growth of the μ Phase (Ni_6Nb_7) in the Ni-Nb System

S.S.K. BALAM, H.Q. DONG, T. LAURILA,
V. VUORINEN, and A. PAUL

Incremental diffusion couple experiments are conducted to determine the average interdiffusion coefficient and the intrinsic diffusion coefficients of the species in the Ni_6Nb_7 (μ phase) in the Ni-Nb system. Further, the tracer diffusion coefficients are calculated from the knowledge of thermodynamic parameters. The diffusion rate of Ni is found to be higher than that of Nb, which indicates higher defect concentration in the Ni sublattice.

In the latest single or polycrystalline Ni-based superalloys, significant proportions of refractory elements such as niobium, molybdenum, and tungsten are added to enhance the high-temperature performance of the alloy. However, during exposure at high temperatures and pressures, topological-close-packed (tcp) compounds such as the μ, σ, and Laves phases nucleate and grow.[1–6] Owing to their poor mechanical properties, the presence of tcp phases degrades the tensile and creep properties of Ni-based superalloys significantly.[3] Moreover, the loss of alloying elements from the matrix may also lead to chemical degradation.[2,3]

Many studies have concentrated on the development of the Nb-Ni phase diagram. Despite the extensive work done on the system, confusion still exists over the composition range of some of the phases.[7–19] Since diffusion plays a major role on the growth of these phases in the superalloys, understanding of the diffusion mechanisms would provide considerable insight into the development of microstructures in Ni-based superalloys. However, very little has been done to understand the diffusion mechanism. Sluiter et al.[20] studied the site occupancy in the μ phase in this system in order to obtain a clearer view about the possible atomic diffusion mechanisms. Further, Sprengel et al.[21,22] studied the growth kinetics and calculated the interdiffusion coeffi-

cient of the phases. They studied interdiffusion by using the diffusion couple technique where the end members were made of pure elements. Consequently, both the intermetallic compounds Ni_3Nb and the Ni_6Nb_7-μ grew together under these circumstances. It should be noted that the interdiffusion coefficient $\tilde{D}$ in Ni_3Nb, as calculated in References 21 and 22, did not change systematically with temperature, which can be regarded as an experimental error. Since, in multiphase diffusion, the growth of one phase is dependent on the growth of other phases, it is likely that the value of $\tilde{D}$ calculated in Ni_6Nb_7-μ phase was also affected by this error. Moreover, there is no knowledge about the intrinsic diffusion coefficient of the species. Hence, there is a clear need to obtain quantitative diffusion kinetic data on the growth of IMCs in the Nb-Ni system.

The aim of the present work is to calculate the intrinsic and interdiffusion coefficient from incremental diffusion couple experiments in the Ni_6Nb_7 μ phase. The composition of the end members of a diffusion couple is chosen such that only one phase grows in the interdiffusion zone. This helps to avoid any errors one might introduce because of the presence other phases in the interdiffusion zone. A further objective is to calculate the activation energy for diffusion, which provides information about the atomic mechanism of diffusion and helps in predicting the defect structure of the compounds. Surprisingly, to date, there are hardly any data available on mobilities of the species in these TCP compounds.

In this study, an incremental diffusion couple technique was used to determine the diffusion parameters owing to the reasons discussed previously. Ni and Nb with 99.95 wt pct purity supplied by Alfa Aesar (Ward Hill, MA) were used to fabricate the samples. The Nb59 at. pct Ni alloy was prepared in an arc melting furnace and then homogenized at 1373 K (1100 °C) for 50 hours. Subsequently, pieces with 6×6 mm^2 cross section and 1-mm thickness were cut from the alloy and coupled with pure Nb of similar dimensions. Bonding faces of the couple halves were ground with emery papers and polished with 0.25-μm alumina slurry. To finalize the sample preparation, the polished surfaces were cleaned ultrasonically in ethanol and dried in hot air. The bonding halves were clamped with minimum pressure required in a special fixture to allow good contact between the bonding surfaces. Experiments were conducted in vacuum (~10^{-7} kPa) in the temperature range of 1273 K to 1423 K (1000 °C to 1150 °C) for fixed annealing time 25 hours. The temperature was controlled within ±5 °C. Prior to annealing, particles of titanium dioxide (TiO_2) were introduced as the Kirkendall markers at the bonding interface. The oxide powder with particle size of ~1 μm was dispersed in acetone and then applied onto the bonding surfaces before joining.

After standard metallographic sample preparation, cross sections of annealed diffusion couples were examined in a scanning electron microscope and composition profiles of the interdiffusion zone were measured using an energy-dispersive X-ray spectrometer. The position of the Kirkendall marker plane was monitored with the presence of the X-ray peak of Ti.

S.S.K. BALAM, Postgraduate Student, and A. PAUL, Associate Professor, are with the Department of Materials Engineering, Indian Institute of Science, Bangalore 560012, India. Contact e-mail: aloke.paul@materials.iisc.ernet.in H.Q. DONG, Postgraduate Student, T. LAURILA, Docent, and V. VUORINEN, Senior Lecturer, are with the Department of Electronics, Faculty of Electronics, Communication and Automation, Aalto University School of Science and Technology, Espoo, Finland.
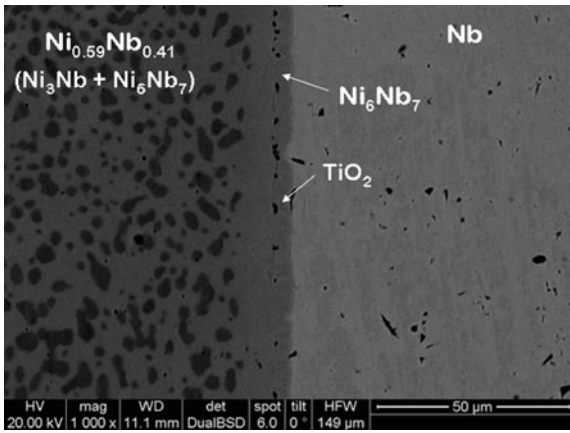
(a)
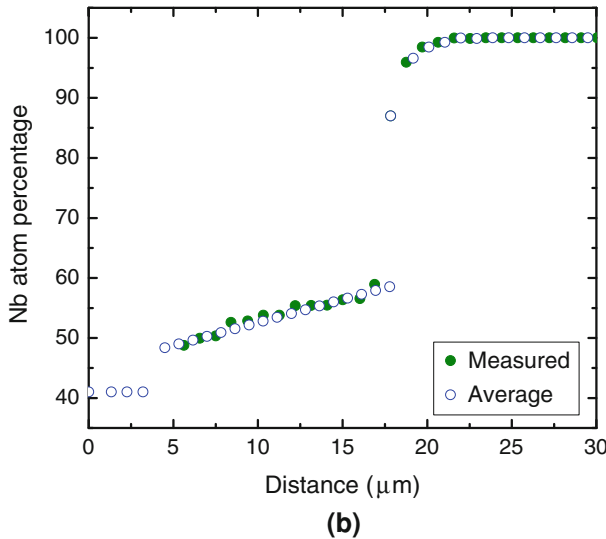
(b)

Fig. 1—(a) Interdiffusion zone developed at 1373 K (1100 °C) annealed for 25 h in the (Nb59 at. pct Ni)/Nb diffusion couple and (b) corresponding composition profile.

Figure 1(a) shows a scanning electron micrograph of the interdiffusion zone that developed during annealing at 1323 K (1050 °C). Figure 1(b) shows the corresponding measured and the average composition profile considered in the calculations. It is to be noted that confusion over the composition range of the phases in this system still exist. Our composition profile, however, matches well with the composition range proposed by Joubert et al.,[15] as shown in Figure 2, compiled by Okamoto.[17]

The interdiffusion coefficient, $\tilde{D}$, is calculated following Wagner's[23] relation expressed as

$$\tilde{D}(Y^*) = \frac{V_m}{2t}\left(\frac{dx}{dY}\right)^* \left[(1-Y^*)\int_{-\infty}^{x^*}\frac{Y}{V_m}dx + Y^*\int_{x^*}^{\infty}\frac{1-Y}{V_m}dx\right]$$

[1]

where the asterisk represents the position of interest, x is the position parameter, and Y is expressed as $\frac{N_i - N_i^-}{N_i^+ - N_i^-}$,

where N_i is the mole fraction of component i. The superscripts + and – refer to the mole fractions at the unreacted left-hand ($x = -\infty$) and right-hand ($x = +\infty$) ends of the couple, respectively, and V_m is the molar volume. The molar volume of Nb and the μ phase are calculated as 10.82×10^{-6} and 8.53×10^{-6} m^3/mol, from the lattice parameter data available in the literature.[24] The average molar volume of the alloy (Nb59 at. pct Ni) is calculated as 8.09×10^{-6} m^3/mol from the volume fraction of the phases and their respective molar volumes. The molar volume of the Ni$_3$Nb phase is considered as 7.49×10^{-6} m^3/mol. It was noticed that there were hardly any changes in the value of $\tilde{D}^\mu$ with composition, a fact also found by Sprengel et al.[22] The average value calculated is shown in Figure 3 with respect to Arrhenius equation expressed as

$$\tilde{D}^\mu = \tilde{D}_0 \exp\left(-\frac{Q}{RT}\right)$$

[2]

where $\tilde{D}_0$ is the pre-exponential exponent and Q is the activation energy. The activation energy calculated using Eq. [2] is found to be 319 ± 7 kJ/mol. The activation energy calculated by Sprengel et al.[22] was found to be 271 kJ/mol. When considering the difference in these values, it should be noted that the present value was determined using incremental diffusion couples, whereas that of Sprengel et al.[22] was calculated from the data obtained by using pure elements as the end members. Thus, in the present case, the effect of other growing phases inside the diffusion zone on the activation energy of Ni$_6$Nb$_7$ was excluded. Although the error percentage is not mentioned by Sprengel et al., our rough estimation indicates that the error in the present calculation is lower than the error in their calculations. It was already mentioned previously that the interdiffusion coefficient $\tilde{D}$ in Ni$_3$Nb calculated by Sprengel et al. did not change systematically with temperature. Ideally, the diffusion coefficient is a material constant. The layer thickness depends on the end-member compositions and the number of phases present in the multiphase interdiffusion zone. The composition profile of the entire interdiffusion zone is important for the calculation of the diffusion parameter in a particular phase. So, in multiphase diffusion, if there is a problem with growth of a particular phase for any reason, calculation of the diffusion parameter in other phases will also be affected. Therefore, we can expect a higher error in calculation of $\tilde{D}$ in the Ni$_6$Nb$_7$-μ phase by Sprengel et al. in the multiphase diffusion zone compared to the data calculated in the present study from an incremental couple.

The intrinsic diffusion coefficient, D_i, of element i in the μ phase is determined at the Kirkendall marker plane (~55 at. pct Nb) detected by the presence of inert TiO$_2$ particles. The inert particles move depending on the relative mobilities of species. The ratio of diffusivities of the elements can be calculated at the composition corresponding to the Kirkendall marker plane using the relation developed by van Loo:[25]
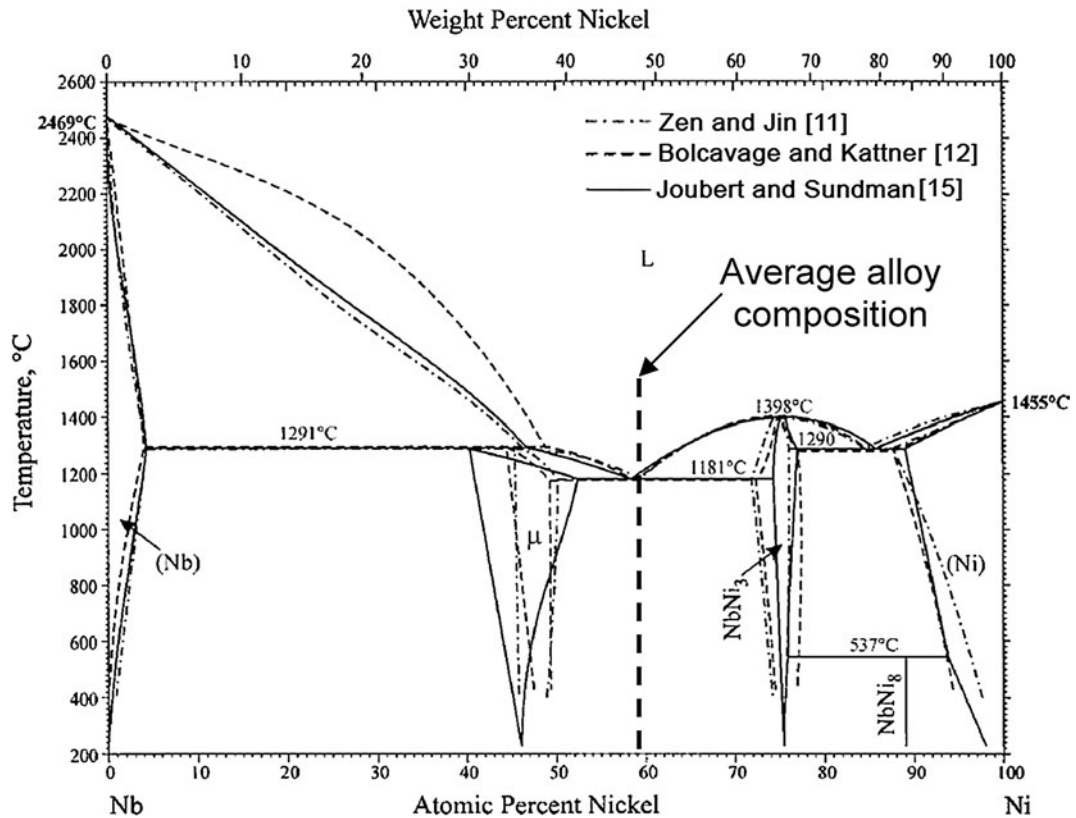
Fig. 2—Ni-Nb phase diagram compiled by Okamoto.[17] Dotted line shows the average composition of the alloy prepared to the couple with pure Nb.
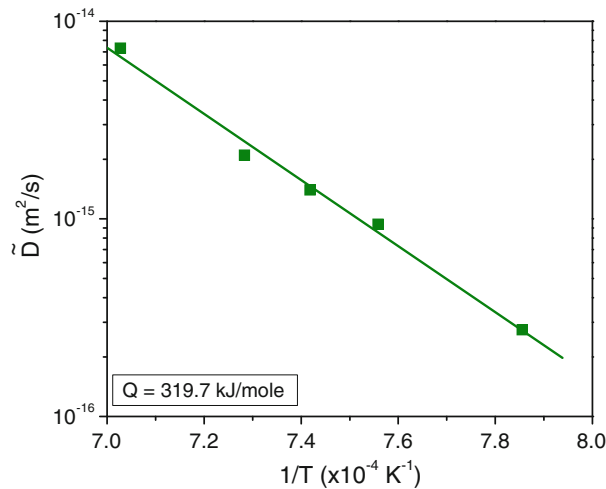

Fig. 3—Average $\tilde{D}$ of the μ phase calculated at different temperatures.

$$\left.\frac{D_{Ni}^{\mu}}{D_{Nb}^{\mu}}\right|_{55at.pct} = \frac{V_{Ni}}{V_{Nb}}\left[\frac{N_{Ni}^{+}\int_{-\infty}^{x_K}\frac{Y}{V_m}dx - N_{Ni}^{-}\int_{x_K}^{\infty}\frac{(1-Y)}{V_m}dx}{-N_{Nb}^{+}\int_{-\infty}^{x_K}\frac{Y}{V_m}dx + N_{Nb}^{-}\int_{x_K}^{\infty}\frac{(1-Y)}{V_m}dx}\right] \quad [3]$$

Here, V_{Ni} and V_{Nb} are the partial molar volume of the species Ni and Nb at the composition of interest that is at the Kirkendall marker position. Because of the lack

of knowledge on the change in lattice parameter and molar volume with composition in the μ phase, we assume that $V_{Ni} = V_{Nb} = V_m^{\mu}$. It should be noted that some error could be introduced because of this assumption. For example, the ratio of the partial molar volume of the species, $\frac{V_{Mo}}{V_{Co}}$, is around $2^{[26]}$ in the μ phase. Further, D_{Ni}^{μ} and D_{Nb}^{μ} are the intrinsic diffusion coefficients at the composition of interest, calculated from the knowledge of $\tilde{D}$ and the ratio of intrinsic diffusivities by using[25]

$$\tilde{D}^{\mu} = C_{Ni}V_{Ni}D_{Nb}^{\mu} + C_{Nb}V_{Nb}D_{Ni}^{\mu} \quad [4]$$

Here, C_{Ni} and C_{Nb} are the concentrations of elements Ni and Nb, respectively. Since we have assumed $V_{Ni} = V_{Nb} = V_m^{\mu}$ and concentration is expressed as $C_i = N_{Ni}/V_m$, Eq. [4] can be written

$$\tilde{D}^{\mu} = N_{Ni}D_{Nb}^{\mu} + N_{Nb}D_{Ni}^{\mu} \quad [5]$$

The ratio of the intrinsic diffusion coefficient of the elements, $\frac{D_{Ni}^{\mu}}{D_{Nb}^{\mu}}$, was found to be in the range of 3.84 to 4.76 at different temperatures. It should be noted that the ratio calculated different temperatures are more or less the same. The change in intrinsic diffusion of elements at different temperatures is presented in Figure 4(a).

The diffusion couple technique is considered as an indirect but reliable method to determine the tracer
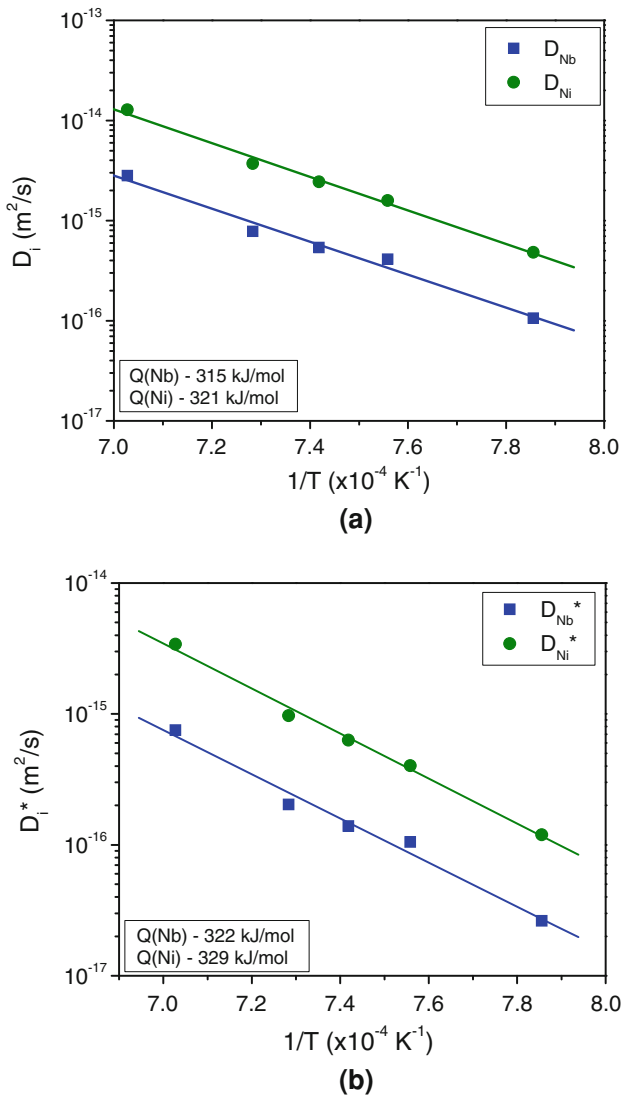
Fig. 4—(a) Intrinsic diffusion coefficients and (b) tracer diffusion coefficients of elements in the μ phase.

1373 K, and 1423 K (1000 °C, 1050 °C, 1075 °C, 1100 °C, and 1150 °C), respectively. The D_i^* values of elements calculated at 55 at. pct at different temperatures are presented in Figure 4(b).

There is not much difference in the activation energy for diffusion of elements and the margin mainly comes from the difference in the pre-exponential factor. Although the number of Nb atoms is higher than that of Ni atoms, the faster diffusion rate of Ni indicates that the concentration of defects in the Ni sublattice must be higher than that of the defects in the Nb sublattice. In fact, a similar trend was noticed in the μ phase in the Co-Mo system. The diffusion rate of Mo was found to be higher in the Co_7Mo_6 μ phase.[25] On the other hand, Fe had a faster diffusion rate in the Fe_7Nb_6 μ phase in the Fe-Nb system,[28] where the number of Fe atoms is higher than Nb. The diffusion process in ordered phases is very complicated, because it depends on the presence of antisites and vacancies. Moreover, the concentration of these defects was not necessarily the same on different sublattices. To date, only Ni-Al[29–31] is studied extensively where diffusion of different elements in intermetallic compounds is discussed with the help of defect concentrations calculated on different sublattices. The crystal structure of the m phase is more complicated compared to the β and γ phases in the Ni-Al system. There is an effort to understand the diffusion process with respect to the defects available in other systems.[32] Data calculated in this study will help in understanding the atomic mechanism of diffusion and validate theoretical calculations on defect concentrations in the μ phase.

diffusion coefficient of elements, D_i^*.[27] The D_i^* are related with D_i following the relation[25]

$$D_{Ni}^{\mu} = D_{Ni}^* \frac{V_m^{\mu}}{V_{Nb}} \frac{d \ln a_{Ni}}{d \ln N_{Ni}} W = D_{Ni}^* \frac{d \ln a_{Ni}}{d \ln N_{Ni}} \quad [6a]$$

$$D_{Nb} = D_{Nb}^* \frac{V_m^{\mu}}{V_{Ni}} \frac{d \ln a_{Nb}}{d \ln N_{Nb}} W = D_{Nb}^* \frac{d \ln a_{Nb}}{d \ln N_{Nb}} \quad [6b]$$

where a_i is the activity of element i; $\frac{d \ln a_{Ni}}{d \ln N_{Ni}} = \frac{d \ln a_{Nb}}{d \ln N_{Nb}}$ is the thermodynamic factor; and W is the vacancy wind effect, which is difficult to calculate because of the complicated crystal structure of the μ phase. It has already been shown that the contribution of W, in general, can be neglected (that means $W \approx 1$). Further, we assumed earlier that $V_{Ni} = V_{Nb} = V_m^{\mu}$. The thermodynamic factor was calculated at 55 at. pct on the basis of a thermodynamic assessment,[15] yielding 4.03, 3.93, 3.88, 3.84, and 3.74 at 1273 K, 1323 K, 1348 K,

REFERENCES

1. J.X. Yang, Q. Zheng, X.F. Sun, H.R. Guan, and Z.Q. Hu: *Mater. Sci. Eng. A*, 2007, vol. 465A, pp. 100–08.
2. M. Simonetti and P. Caron: *Mater. Sci. Eng. A*, 1998, vol. 254A, pp. 1–12.
3. R.C. Reed and C.M.F. Rae: *Acta Mater.*, 2001, vol. 49, pp. 4113–25.
4. Y.H. Kong and Q.Z. Chen: *Mater. Sci. Eng. A*, 2004, vol. 366A, pp. 135–43.
5. S. Petronić and A. Milosavljević: *FME Trans.*, 2007, vol. 35, pp. 189–93.
6. S.H.M. Anijdan and A. Bahrami: *Mater. Sci. Eng. A*, 2005, vol. 396A, pp. 138–42.
7. L. Kaufman and H. Nesor: *CALPHAD*, 1978, vol. 2, pp. 82–108.
8. K.J. Zeng, X.Z. Zeng, and Z.P. Jin: *J. Alloys Compd.*, 1992, vol. 179, pp. 177–85.
9. K.J. Zeng and Z.P. Jin: *Scripta Metall. Mater.*, 1992, vol. 26, pp. 417–22.
10. H. Okamoto: *J. Phase Equilib.*, 1992, vol. 13, pp. 444–45.
11. K. Zen and Z. Jin: *Scripta Metall. Mater.*, 1992, vol. 26, pp. 417–22.
12. A. Bolcavage and U.R. Kattner: *J. Phase Equilib.*, 1996, vol. 17, pp. 92–100.
13. H. Okamoto: *J. Phase Equilib.*, 1998, vol. 19, p. 289.
14. J.M. Joubert and Y. Feutelais: *CALPHAD*, 2002, vol. 26, pp. 427–38.
15. J.M. Joubert, B. Sundman, and N. Dupin: *CALPHAD*, 2004, vol. 28, pp. 299–306.
16. H.L. Chen, Y. Du, H.H. Xu, Y. Liu, and J.C. Schuster: *J. Mater. Sci.*, 2005, vol. 40, pp. 6019–22.
17. H. Okamoto: *J. Phase Equilib. Diff.*, 2006, vol. 27, p. 314.
18. H. Chen and Y. Du: *CALPHAD*, 2006, vol. 30, pp. 308–15.
19. H. Okamoto: *J. Phase Equilib. Diff.*, 2008, vol. 29, p. 210.

20. M.H.F. Sluiter, A. Pasturel, and Y. Kawazoe: *Phys. Rev. B*, 2003, vol. 67, pp. 174203-1–174203-10.
21. W. Sprengel, M. Denkinger, and H. Mehrer: *Intermetallics*, 1994, vol. 2, p. 127.
22. W. Sprengel, M. Denkinger, and H. Mehrer: *Intermetallics*, 1994, vol. 2, p. 137.
23. C. Wagner: *Acta Metall.*, 1969, vol. 17, p. 99.
24. W.B. Pearson: *Handbook of Lattice Spacings and Structures of Metals and Alloys*, Pergamon Press, Oxford, United Kingdom, 1967.
25. F.J.J. van Loo: *Prog. Solid State Chem.*, 1990, vol. 20, p. 47.
26. V.D. Divya, U. Ramamurty, and A. Paul: *Intermetallics*, 2010, vol. 18, p. 259.
27. A. Paul, A.A. Kodentsov, and F.J.J. van Loo: *J. Alloys Compd.*, 2005, vol. 403, p. 147.
28. S.S.K. Balam and A. Paul: *Metall. Mater. Trans. A*, 2010, vol. 41A, p. 2175.
29. H. Numakura, T. Ikeda, M. Koiwa, and A. Almazouzi: *Phil. Mag.*, 1998, vol. 77, p. 887.
30. H. Numakura, T. Ikeda, H. Nakajima, and M. Koiwa: *Mater. Sci. Eng. A*, 2001, vol. 312, p. 109.
31. St. Frank, S.V. Divinski, U. Södervall, and C. Herzig: *Acta Mater.*, 2001, vol. 49, p. 1399.
32. X.Y. Zhang, W. Sprengel, K. Blaurock, A.A. Rempel, K.J. Reichle, K. Reimann, H. Inui, and H.E. Schaefer: *Phys. Rev. B*, 2002, vol. 66, p. 144105.